

Field-controlled magnetic phase separation in $(\text{La}_{0.25}\text{Pr}_{0.75})_{0.7}\text{Ca}_{0.3}\text{Mn}^{18}\text{O}_3$ probed by ^{55}Mn NMR

A. Gerashenko,^{1,2} Y. Furukawa,¹ K. Kumagai,¹ S. Verkhovskii,² K. Mikhalev,² and A. Yakubovskii³

¹*Division of Physics, Graduate School of Science, Hokkaido University, Sapporo 060-0810, Japan*

²*Institute of Metal Physics, Ural Branch of Russian Academy of Sciences, Ekaterinburg GSP-170, Russia*

³*Russian Research Centre Kurchatov Institute, Moscow 123182, Russia*

(Received 20 September 2002; revised manuscript received 17 December 2002; published 12 May 2003)

The influence of the ^{16}O - ^{18}O isotope substitutions on magnetic state of perovskite-type manganite $(\text{La}_{0.25}\text{Pr}_{0.75})_{0.7}\text{Ca}_{0.3}\text{MnO}_3$ is studied by ^{55}Mn NMR. Successive cycling with an isochronal exposure at different magnetic fields up to $H=8T$ is used to study the field-induced transition from antiferromagnetic insulating (AFI) state to the ferromagnetic metal (FMM) one in the ^{18}O -enriched sample. After exposure at $H > H_{cr} \sim 5.3T$ the NMR spectrum of the ^{18}O sample provides evidence for a magnetic phase separation (PS) into the coexisting AFI and FMM domains. Further increase of exposing field leads to a progressive growth of the FMM phase at the expense of AFI domains. Its relative fraction can be controlled by external magnetic field and the resulting magnetic structure in the PS region is discussed. Anomalous T dependence of the ^{55}Mn nuclear spin-lattice relaxation rate is revealed in the FMM state of both ^{16}O - and ^{18}O -enriched samples. The possible influence of the Pr magnetic ordering at $T \sim 40$ K on the spin-lattice relaxation is considered.

DOI: 10.1103/PhysRevB.67.184410

PACS number(s): 75.47.Gk, 75.25.+z, 76.60.Jx

I. INTRODUCTION

Perovskite-type manganites $R_{1-x}\text{M}_x\text{MnO}_3$ ($R=\text{La}, \text{Pr}$ is a trivalent rare-earth ion) are subjected to extensive studies after observation of a ‘‘colossal’’ negative magnetoresistance (CMR) effect for $0.2 < x < 0.4$. The CMR effect is related closely in physics to phase transition from the charge ordered antiferromagnetic insulating (CO AFI) state to the ferromagnetic metal (FMM) one.¹ Thermal hysteresis revealed in transport and magnetic properties of these compounds evidences the first-order transition accompanied by the phase separation (PS) into CO AFI and FMM domains.² An ionic state of Mn determines unambiguously its spin configuration. The $\text{Mn}^{4+}/\text{Mn}^{3+}$ charge order is accompanied by substantial polaronic effects³ and the Jahn-Teller-type lattice distortions⁴ in the sublattice of the MnO_6 octahedra and it defines in many respects the microstructure of magnetic state in a low-temperature phase.

The $(\text{La}_y\text{Pr}_{1-y})_{0.7}\text{Ca}_{0.3}\text{MnO}_3$ manganite is one of the most convenient systems for studying the PS phenomenon. Recently^{5,6} it was shown that the ground state of electron system becomes extremely unstable at $y \sim 0.25$ and even the isotopic substitution of ^{16}O by ^{18}O influences significantly the transport and magnetic properties of this compound. On cooling down in zero external magnetic field (ZFC), the $(\text{La}_{0.25}\text{Pr}_{0.75})_{0.7}\text{Ca}_{0.3}\text{MnO}_3$ sample with ^{16}O isotope (referred below as LPCMO¹⁶) shows the successive transitions to the CO state at $T < T_{co} = 180$ K, to the AF state below $T_N = 150$ K, and finally to the FMM one below $T_c = 120$ K. On the other hand, the ^{18}O -enriched sample (LPCMO¹⁸) remains in the AFI state down to the very low temperature under ZFC conditions. However, this AFI ground state is extremely unstable and can be easily transformed to the FMM one with the same saturation magnetization as in the LPCMO¹⁶ by applying external magnetic field above the critical value H_{cr} .

The detailed magnetic phase diagram of LPCMO¹⁸ in a wide range of H and T has been reported as a result of magnetization studies.⁷ It was shown that the AFI-FMM phase composition in the PS region above $H_{cr}(T)$ is controlled by magnetic field. Any prescribed ratio of AFI to FMM phases can be obtained in the PS region and might be frozen by the decrease of the magnetic field below the critical value H_{cr} . The new phase composition depends on neither time nor magnetic-field variations below H_{cr} . The microscopic evidence of the phase transition from AFI to FMM state in LPCMO¹⁸ was obtained from ^{139}La NMR studies at 5K.⁷ Two well-resolved ^{139}La NMR lines corresponding to AFI and FMM domains were clearly observed and their relative intensities determine directly the fraction of both the phases in the PS region.

However, ^{139}La NMR spectra are not informative as to the short-range CO of the Mn ions in the AFI phase. A local magnetic field $^{139}H_{loc}$ probed by the ^{139}La is mainly due to the overlap of $\text{La}(6s)$ and $\text{Mn}(t_{2g})$ orbitals, so a contribution of holes located at the e_g orbital of Mn^{3+} ions is greatly reduced in the AFI state.⁸ Thus the position of the ^{139}La NMR signal in the AFI state is not sensitive to a valence state of the nearest Mn ions. In sharp contrast, one may expect that ^{55}Mn NMR study allows getting a more detailed information about the charge and magnetic states of Mn ions in the AFI phase.

In this paper, we present the results of the ^{55}Mn NMR studies of the field-controlled PS in $(\text{La}_{0.25}\text{Pr}_{0.75})_{0.7}\text{Ca}_{0.3}\text{MnO}_3$ with different oxygen isotope content to get better insight in the microstructure of the AFI ground state. The temperature dependence of nuclear spin-lattice relaxation rate is studied in the FMM state with special care of finding the microscopic evidence for magnetic ordering of Pr ions.

II. EXPERIMENT

The ceramic sample preparation and isotope enrichment procedures for $(\text{La}_{0.25}\text{Pr}_{0.75})_{0.7}\text{Ca}_{0.3}\text{MnO}_3$ studied in this

work were described in detail in Ref. 5. Oxygen isotope content in the samples prepared from the same starting pellet was ^{16}O -100% (LPCMO 16) and ^{18}O -85%; ^{16}O -15% (LPCMO 18). The NMR measurements were performed with a home-built pulse phase-coherent NMR spectrometer operated in the frequency range up to 450 MHz using spin-echo technique. The NMR spectra were obtained by measuring at each frequency an intensity of the Hahn spin-echo signal. The width of a $\pi/2$ rf pulses does not exceed $1.5\text{--}2\mu\text{s}$. The amplitude of the exciting rf pulses was optimized for the maximum of echo signal in measuring each individual line in the NMR spectrum. Any variations of the receiver gain including rf coupling with resonant circuit were taken into account in measurement of the line intensity using an additional calibration rf pulse with fixed amplitude formed in the rf coil after echo signal at each frequency point. The original probe head designed for ^{55}Mn NMR allowed to measure spectra in the range of 180–450 MHz using a single rf coil. The ^{55}Mn NMR spectrum measurements were performed in zero magnetic field (ZFNMR) and in external magnetic field up to 8 T at $T=1.5$ K. The field-cycling (fc) procedure (ZF $\rightarrow H_{fc} \rightarrow$ ZF) was performed as follows: after ZFC the external magnetic field was increased up to H_{fc} and was kept fixed for about $t_{\text{exp}} \sim 20$ min to exclude the transition effects. Then the magnetic field was switched off and the ZFNMR spectrum was measured.

III. RESULTS AND DISCUSSIONS

Figure 1(a) shows the ^{55}Mn ZFNMR spectra in the FMM state in LPCMO 16 after ZFC. It presents a single line peaked near $\nu \approx 380$ MHz. The line shows a strong rf enhancement $\eta \approx 100$ which is typical for ordered FM. On the other hand, in the AFI state of the LPCMO 18 sample after ZFC, the observed spectrum is quite different, as shown in Fig. 1(e). The main peak is observed around 317 MHz, where a large rf power is needed for the signal detection in contrast to the signals from the FMM state, while the small peak around 380 MHz, with a large rf enhancement is also detected. Besides the rf enhancement factors the other characteristics of NMR signals for these two peaks are also completely different. Nuclear-spin-spin relaxation time $T_2 = 10(5)\mu\text{s}$ ($T = 1.5\text{K}$) and nuclear spin-lattice relaxation time $T_1 = 2.9$ ms at the main peak are much shorter than the corresponding $T_2 \sim 100\mu\text{s}$ and $T_1 \sim 1$ s observed at the smaller one. These short relaxation times are typical for AFI state in manganites. Thus, we attribute the peak around 380 MHz to ^{55}Mn NMR in the FMM phase while that around 317 MHz is assigned to the AFI phase. The same lines with the same assignment were reported earlier for the half-doped $\text{La}_{0.5}\text{Ca}_{0.5}\text{MnO}_3$ (Ref. 9) and $\text{Pr}_{0.5}\text{Sr}_{0.5}\text{MnO}_3$.¹⁰ It is interesting that in the parent CaMnO_3 slightly doped by Pr the peak of FMM-line shifts down to 300 MHz as reported in Ref. 11.

Figures 1(b,c,d) show the H_{fc} dependence of the ^{55}Mn ZFNMR spectrum measured with the field cycling method described above. As shown in the figures, with increasing H_{fc} , the peak around 317 MHz originated from the AFI phase gradually disappears, while a relative intensity of the peak around 380 MHz (FMM phase) grows up. Finally, the

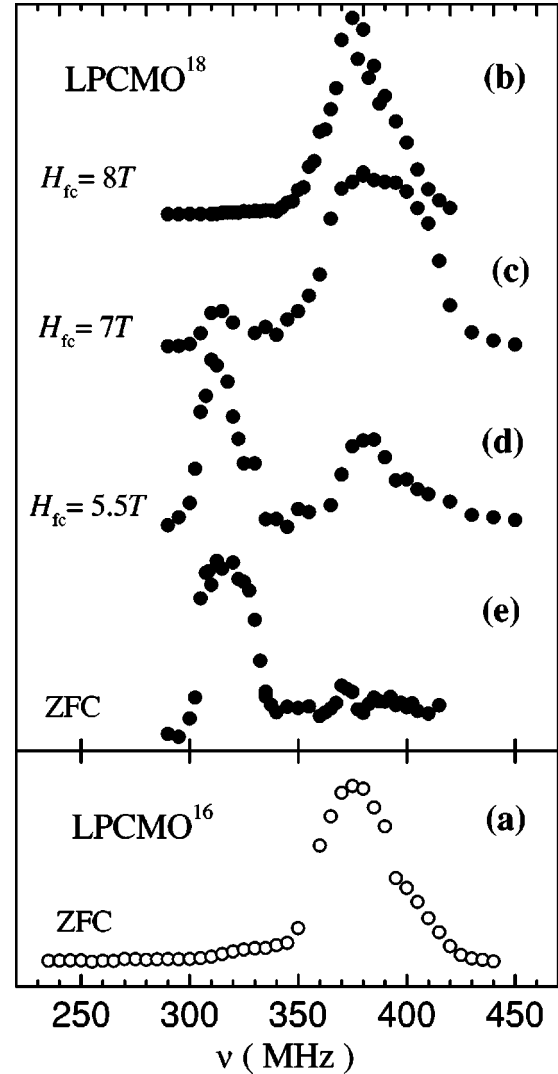


FIG. 1. ^{55}Mn ZFNMR spin-echo spectra of LPCMO 18 (solid circles) and LPCMO 16 (open circles). Spectra were measured at the polycrystalline powder after primary ZFC cooling down to $T = 1.5$ K and subsequent isochronal magnetic-field circling $H=0 \rightarrow H_{fc} \rightarrow H=0$ with $H_{fc}=0\text{T}$ —(a) and (e), 8 T—(b), 7 T—(c), 5.5 T—(d).

spectrum in the LPCMO 18 after exposing to $H_{fc} = 8$ T [Fig. 1(b)] becomes very similar to that in the FMM state of the LPCMO 16 Fig. 1(a). From the comparison of FMM signal intensities between the virgin (ZFC) and the final (exposing to $H_{fc} = 8\text{T}$) states, the minor FMM phase in the virgin LPCMO 16 sample can be estimated at most a few percents. In the estimation of the AFI/FMM line intensities, the following points were taken into account. We found unchanged both the rate of the ^{55}Mn echo decay T_2 and the rf enhancement factor for the corresponding lines after applying field cycling at different H_{fc} . Moreover, only intensities, not the resonance, frequencies, of the peaks changed during this field-cycling procedure. So in our spin-echo experiments with the fixed optimal both $\pi/2$ rf-pulse and the rf power gain, one proves that only the change in concentrations of the two defined magnetic phases were traced.

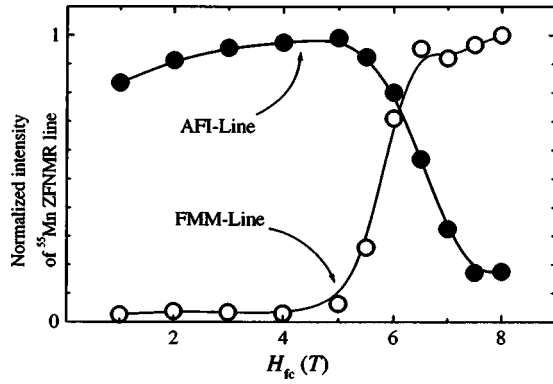


FIG. 2. The relative intensity of ^{55}Mn ZFNMR line in the AFI domains ($\nu \sim 317$ MHz, solid circles) and the FMM domains ($\nu \sim 380$ MHz, open circles) measured at $T = 1.5$ K for LPCMO¹⁸ after subsequent isochronal magnetic-field cycling at H_{fc} . The intensities are normalized to the corresponding maxima. The corrections for the transverse relaxation and enhancement factor are taken into account as explained in the text.

The amount of AFI or FMM phases is proportional to intensity of the corresponding ZFNMR line measured at $T = 1.5$ K after subsequent field cycling at different H_{fc} . The relative intensities of the AFI (●) or FMM (○) lines normalized to their maximum are shown in Fig. 2 for the virgin (ZFC) LPCMO¹⁸. With increase in H_{fc} , the amount of AFI domains increases slightly below $H_{fc} \sim 5T$, then starts to decrease nearly to zero at $H_{fc} = 8T$. On the other hand, the amount of FMM domains increases strongly above $H_{fc} \sim 5T$ and saturates at $H_{fc} \sim 7T$. In the region between $\sim 5.5T$ and $7T$, the AFI and FMM domains coexist in LPCMO¹⁸, indicating the microscopically inhomogeneous magnetic phase separation. These ^{55}Mn -NMR results provide a microscopic confirmation of the inhomogeneous PS in LPCMO¹⁸ in the region where a detailed balance of the volume fractions of the AFI and the FMM phases can be controlled by external magnetic field. The present results are consistent with H - T magnetic phase diagram obtained by magnetization measurements and ^{139}La NMR studies.⁷

In order to shed light on more details of the electronic and magnetic states of Mn ions in FMM phase, we have investigated the external magnetic-field dependence of the ^{55}Mn NMR spectra. Figure 3 shows the H dependences of ^{55}Mn NMR spectrum measured in LPCMO¹⁶ at $T = 4$ K (open circles) and of the spectrum for saturated FMM LPCMO¹⁸ corresponding to Fig. 1(b). With increase in H the peak frequencies for both the samples shift to lower frequency according to the relation $\Delta\nu(\text{MHz}) \sim 10.1H(\text{T})$ as shown in the inset of Fig. 3. This value is in agreement with the gyromagnetic ratio of ^{55}Mn nucleus ($^{55}\gamma/2\pi = 10.50$ T/MHz) within our experimental accuracy. Since the hyperfine field H_{hf} at the Mn sites is mainly originated from the core-polarization contribution, its direction is opposite to that of the Mn spin moment. This result suggests that all the Mn spin moments in the FMM state aligned along the H direction without any canting. H_{hf} is proportional to $A_{hf}\langle S \rangle$, where A_{hf} is a hyperfine coupling constant and $\langle S \rangle$ is the spin moment. Combining the experimental value of H_{hf}

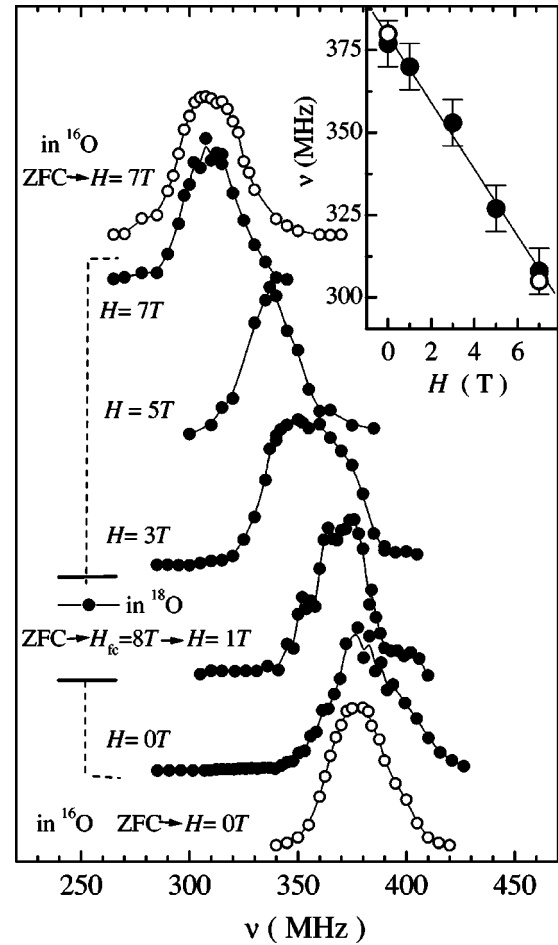


FIG. 3. H -dependence of ^{55}Mn spin-echo spectra measured at $T = 4$ K for FMM phase of LPCMO¹⁶ (open circles) and LPCMO¹⁸ (solid circles) samples. The ZFC LPCMO¹⁸ sample was transformed to FMM state by exposing at $H_{fc} = 8T$. The line is a guide for eye. The inset shows the frequency of the NMR line peak ν vs H , a slope of solid fitting line corresponds to $\Delta\nu/\Delta H = 10.1$ MHz/T.

$= 36T$, $A_{hf} \approx -100$ kOe/ μ_B (Ref. 12) and the magnetization data measured in the same sample LPCMO¹⁶, the average magnetic moment on the Mn site is estimated as $3.6\mu_B$. This value suggests that the valence of Mn ions in the FMM state can be given to $\text{Mn}^{3.6+}$ in high spin states in ionic approximation; namely, some averaged value between Mn^{4+} ($S = 3/2$) and Mn^{3+} ($S = 2$). This in turn suggests that the electronic state of 0.6 electrons on the e_g orbitals in FMM state must be responsible for metallic conductivity. It should be pointed out that the observation of only one component of the Mn NMR spectrum in the FMM state indicates that the inverse of the lifetime of the electron spins is higher than the NMR frequency [in the exchange narrowing limit between Mn^{4+} ($S = 3/2$) and Mn^{3+} ($S = 2$)].

On the other hand, for the CO AFI phase, we would expect two ^{55}Mn NMR signals from Mn^{4+} ($S = 3/2$) and Mn^{3+} ($S = 2$) ions, because e_g electrons of Mn^{3+} are expected to localize in the AFI state. However, we observed only one signal around 317 MHz corresponding to $H_{hf} \sim 30.2T$. The magnetic moment of the Mn ions in the AFI state is sug-

gested to be smaller than that of the $\text{Mn}^{3,6+}$ ions in the FMM state. Furthermore, the value of $H_{hf} \sim 30.2T$ is well consistent with a theoretical estimation¹⁵ of the on-site hyperfine magnetic field for the Mn^{4+} ion in the crystal field of octahedron symmetry $H_{hf}(\text{Mn}^{4+}) = 30.5T$. Hence, thus this signal can be assigned to Mn^{4+} ions in the CO AFI phase.

As for the NMR signals from Mn^{3+} ions in the CO AFI state, we have not succeeded to find them in the frequency range of 320–450 MHz even with the shortest available delay time ($5 \mu\text{s}$) between rf pulses. This might be due to a much shorter $T_2 < 1 \mu\text{s}$ for Mn^{3+} ions compared to $T_2 \sim 10 \mu\text{s}$ for Mn^{4+} ions in the CO AFI state. A similar negative result was obtained in the ^{55}Mn NMR spin-echo studies of the CO AFI state of $\text{La}_{0.5}\text{Ca}_{0.5}\text{MnO}_3$ (Ref. 9) and $\text{Pr}_{0.5}\text{Sr}_{0.5}\text{MnO}_3$.¹⁰

Finally, we consider peculiarities of the ^{55}Mn nuclear spin-lattice relaxation rate (T_1^{-1}) probing the fluctuations of local magnetic fields in the FMM ordered state of LPCMO¹⁶ (ZFC) and LPCMO¹⁸ (FC at 8 T) samples. The T_1 measurements were performed by saturation-recovery technique in the magnetic fields $H = 1; 2T$ related to the nearly saturated FM spin order of manganese.⁷ The recovery of nuclear magnetization $M_z(t)$ was found nonexponential. It was revealed that the $M_z(t)$ data are not dependent on the parameters of the saturating comb of pulses, so an effect of the restricted spectral spin diffusion on the shape of nuclear magnetization recovery was excluded from consideration. An intrinsic microscopic magnetic inhomogeneity of multicomponent oxide is another source giving rise to a spatial distribution of T_1 (Refs. 14,15) and is resulting in additional term of the stretched exponential form for $M_z(t)$ under condition of the broad-band excitation of the spin system. In our T_1 measurements, only a small part of total ^{55}Mn nuclear spins contributing to the broad FMM line near its peak was available to flip by applying the saturating comb with the pulse duration of 1–2 μs . So we consider that nuclei contributing to the echo signal belong to the species with approximately the same static and fluctuating parts of the local magnetic field and we restrict ourselves in fitting of $M_z(t)$ data by the following standard multiexponential expression given by Ref. 16 for magnetic relaxation of the initially excited central transition in the spin system ($I = 5/2$) with nonequidistantly quadrupole splitted energy spectrum:

$$\frac{M_z(\infty) - M_z(t)}{M_z(\infty)} = \frac{1}{35} \exp\left(-\frac{t}{T_1}\right) + \frac{8}{45} \exp\left(-\frac{6t}{T_1}\right) + \frac{50}{63} \exp\left(-\frac{15t}{T_1}\right). \quad (1)$$

Expression (1) was used for fitting the obtained $M_z(t)$ data.

The T dependence of $1/T_1$ for both ZFC LPCMO¹⁶ (circles) and LPCMO¹⁸ (solid squares) samples cooled down at $H = 8T$ is presented in Fig. 4. It is seen that in the FMM state the temperature behavior of $1/T_1$ is similar for both the samples. With increasing T , T_1^{-1} increases strongly up to $T = 20$ K, have a plateau in the range of $T = 20$ –50 K, and increases again on approaching the transition from the FMM to the AFI state at $T_c = 120\text{K}$. This finding clearly indicates

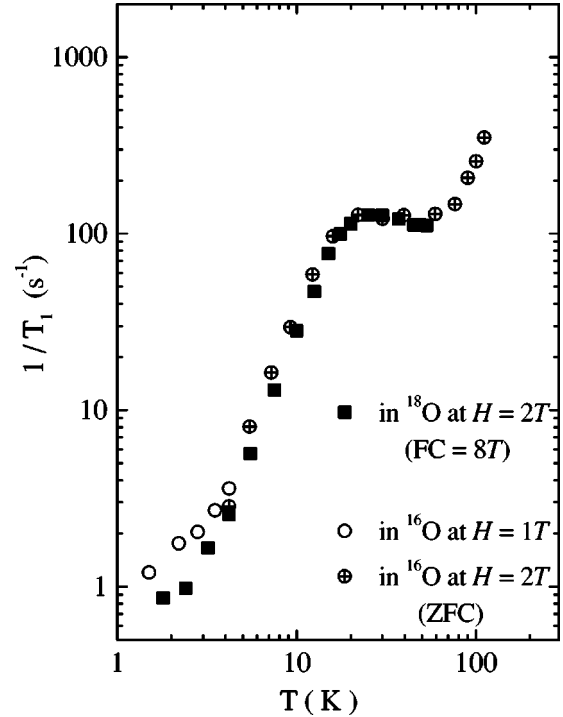


FIG. 4. Temperature dependence of ^{55}Mn nuclear-spin-lattice relaxation rate T_1^{-1} measured in the FMM state of LPCMO¹⁶ and LPCMO¹⁸ samples. The ZFC LPCMO¹⁶ sample was measured in $H = 1T$ (○) and $2T$ (⊕), the LPCMO¹⁸ one was FC in $8T$ and T_1 measurements were performed in $H = 2T$ (■).

that low-frequency fluctuating parts of the local magnetic fields at the Mn sites in the FMM state are not noticeably influenced by oxygen isotope substitution.

As expected at elevated temperatures near T_c , the critical enhancement of magnetic fluctuations at the Larmor frequency of ^{55}Mn nuclei is responsible for a rather strong growth of $(T_1^{-1}) \sim T^3$. On the other hand, T_1^{-1} behavior at low temperature is quite different compared to the exponential rise $^{55}T_1^{-1} \sim \exp(aT)$ (Refs. 9,17) observed for several FM manganites with concentration of mobile holes covering the CMR region of coexisting FM order and metallic conductivity. Similar hump in the temperature dependence of ^{139}La nuclear-spin-lattice rate performed below 100 K for the FM line of ^{139}La of the LPCMO¹⁸ sample FC at $8T$.¹⁸ It is instructive to note that in ferromagnetic metals, the dominating spin-wave contribution to T_1^{-1} via the two-magnon scattering process should lead to the power-law dependence $T_1^{-1}(T) \sim T^\beta$ with β ranging from 2.5 to 1.5 with an increase of the magnon damping.¹⁹

These observations demonstrate a presence of additional magnetic-field fluctuations, which contribute to nuclear-spin-lattice rate of both ^{139}La and ^{55}Mn in FMM state of the studied material. We suppose that the anomalous T_1 behavior at low temperatures is originated from the fluctuating local magnetic field transferred from Pr ion, which should strongly increase around the Pr magnetic ordering temperature. According to the $H-T$ phase diagram⁷ and neutron-diffraction studies⁶ reported for $(\text{La}_{0.25}\text{Pr}_{0.75})_{0.7}\text{Ca}_{0.3}\text{MnO}_3$ with the

very same chemical composition, the magnetic ordering in Pr sublattice occurs at $T_{c,Pr}(H=0) \sim 40$ K, this value being in a good agreement with the observed plateau $20 \sim 50$ K at the $1/T_1$ plot.

The experimental dependence of T_1^{-1} shown in Fig. 4 could be presented as a superposition of two temperature-dependent relaxation mechanisms, one corresponds, roughly, to the activated behavior of the FM ordered Mn moments and the second being induced by freezing of the Pr moments. In fact, this ${}^{55}\text{T}_1^{-1}$ result can be considered as an additional local evidence of the Pr^{3+} magnetic ordering around 40 K. An absence of divergent-like behavior of T_1^{-1} and a presence of rather broad plateau are in favor of the influence of atomic disorder in the Pr/La sublattice on the magnetic ordering due to a rather large distribution of the exchange parameters between the localized electron spins of Pr.

In conclusion, the ${}^{55}\text{Mn}$ NMR spectra of $(\text{La}_{0.25}\text{Pr}_{0.75})_{0.7}\text{Ca}_{0.3}\text{MnO}_3$ show at a microscopic level that the AF order among Mn ions in the LPCMO¹⁸ sample at low temperatures is a metastable magnetic state. After a cycling

of external magnetic field above $H_{cr} \sim 5T$, the field-induced phase transition develops through the nucleation of the FMM phase at the expense of AFI domains. An upper boundary of the AFI-FMM phase separation region is established in the field-cycled NMR experiments and equals to $7.5T$ at $T = 1.5$ K. The ${}^{55}\text{Mn}$ NMR spectrum of the LPCMO¹⁸ sample cooled in the higher magnetic field shows that its magnetic state is just the same as for LPCMO¹⁶, i.e., a long-range FMM. Finally, it is proposed that transferred magnetic coupling between the Mn and Pr spins should be involved into consideration of the unusual low-temperature phase diagram of this manganite.

ACKNOWLEDGMENTS

This study was supported in part by a Grant-in-Aid for scientific research of the Ministry of Education, Culture, Sports, Science and Technology of Japan (A.G.), by Russian Fund for Basic Research under Projects Nos. 99-02-16975, 02-02-16357 and by CRDF Grant No. RP2-2355-MO-02.

¹J.M.D. Coey, M. Viret, and von S. Molnar, *Adv. Phys.* **48**, 167 (1999).

²E.L. Nagaev, *Phys. Usp.* **166**, 833 (1996).

³T. Mizokawa, D.I. Khomskii, and G.A. Sawatzky, *Phys. Rev. B* **63**, 024403 (2001).

⁴J.S. Zhou and J.B. Goodenough, *Phys. Rev. B* **60**, 15 002 (1999).

⁵N.A. Babushkina *et al.*, *Nature (London)* **391**, 159 (1998).

⁶A.M. Balagurov, V.Y. Pomjakushin, D.V. Sheptyakov, V.L. Akse-
nov, N.A. Babushkina, L.M. Belova, A.N. Taldenkov, A.V. Iny-
ushkin, P. Fischer, M. Gutmann, L. Keller, O.Y. Gorbenko, and
A.R. Kaul, *Phys. Rev. B* **60**, 383 (1999).

⁷A. Yakubovskii, K. Kumagai, Y. Furukawa, N. Babushkina, A.
Taldenkov, A. Kaul, and O. Gorbenko, *Phys. Rev. B* **62**, 5337
(2000).

⁸Y. Yoshinari, P.C. Hammel, J.D. Thompson, and S.W. Cheong,
Phys. Rev. B **60**, 9275 (1999).

⁹G. Allodi, R. De Renzi, F. Licci, and M.W. Pieper, *Phys. Rev.
Lett.* **81**, 4736 (1998).

¹⁰G. Allodi, R. De Renzi, M. Solzi, K. Kamenev, G. Balakrishnan
and M.W. Pieper, *Phys. Rev. B* **61**, 5924 (2000).

¹¹M.M. Savosta, P. Novak, M. Marysko, Z. Jirak, J. Hejtmanek, J.
Englich, J. Kohout, C. Martin, and B. Raveau, *Phys. Rev. B* **62**,
9532 (2000).

¹²A.J. Freeman and R.E. Watson, in *Magnetism*, edited by G. T
Rado and H. Suhl (Academic Press, New York, 1965).

¹³T. Kubo *et al.*, *Phys. Soc. Jpn.* **21**, 812 (1966).

¹⁴M.R. McHenry, B.C. Silbernagel, and J.H. Wernick, *Phys. Rev. B*
5, 2958 (1972).

¹⁵N.J. Curro, P.C. Hammel, B.J. Suh, M. Hücker, B. Büchner, U.
Ammerahl, and A. Revcolevschi, *Phys. Rev. Lett.* **85**, 642
(2000).

¹⁶A. Narath, *Phys. Rev.* **162**, 320 (1967).

¹⁷M.M. Savosta, V.A. Borodin, and P. Novak, *Phys. Rev. B* **59**,
8778 (1999).

¹⁸Y. Furukawa (unpublished).

¹⁹V.Yu. Irkhin and M.I. Katsnelson, *Phys. Rev. B* **60**, 14 569
(1999).